Article

J. Mex. Chem. Soc. **2025**, *69*(2)
Regular Issue

ISSN-e 2594-0317

Fabrication of a Highly Sensitive Nanoaptasensor for Rapid and Direct Detection of *Escherichia Coli* (Nasec) in Drinking Water

Elia Velázquez[1,2,3], Oscar Monroy Hermosillo[2], Florina Ramírez Vives[2], Michel Picquart[4], Israel Morales-Reyes[3], Paulina Hernández Garcés[3], Antonio Abad Sánchez[5], Eugenio Gómez Reyes[6], Nikola Batina[*3]

[1]Posgrado en Biotecnología (Ref. 001466), DCBS, UAM-I.
[2]Laboratorio de Tratamiento de Aguas y Microbiología Ambiental, Departamento de Biotecnología, DCBS, UAM-I, CDMX 09340, México.
[3]Laboratorio de Nanotecnología e Ingeniería Molecular, Departamento de Química, DCBI UAM-I, CDMX 09340, México.
[4]Departamento de Física, DCBI, UAM-I, CDMX 09340, México.
[5]Departamento de Diseño Gráfico, CyAD, UAM-A, CDMX 02128, México.
[6]Ingeniería Hidrológica, Departamento de Ingeniería de Procesos e Hidráulica, DCBI, UAM-A, CDMX 09340, México.

***Corresponding author:** Nikola Batina, email: bani@xanum.uam.mx, Tel: +52 55 5804 4939.

Received October 4th, 2023; Accepted Febraury 7th, 2024.

DOI: http://dx.doi.org/10.29356/jmcs.v69i2.2146

Abstract. In this work, a novel nanoaptasensor (NASEc) for rapid and direct detection of *Escherichia coli* (*E. coli*) in drinking water was designed and constructed. The sensor is based on electrical conductivity measurements between a set of bare gold electrodes and a set of modified gold electrodes. The modified electrode set was covered with an aptamer layer (A_{E10}) to improve affinity for *E. coli* and better binding to the electrode surface. Using the modified nanostructured layer with multiwall carbon nanotubes (MWCNT), the high sensitivity of the sensor was achieved and allowed to detect the presence of *E. coli* in quantities of a single colony forming units (CFU) per 100 mL. This sensitivity meets the relevant international drinking water quality standards. Each step in the process of the NASEc fabrication was verified and proved by different analytical techniques at a nanometric and molecular level: UV-vis and Raman Spectroscopy, AFM, and SEM. This portable, simple, and reusable nanoaptasensor with high selectivity and affinity offers faster detection (3 min) in the presence of *E. coli* compared to conventional colony forming units (CFU) counting-based methods (24 to 48 h). NASEc is designed for direct measurements without any pretreatment of samples and is helpful in potable water within a conductivity range of 50 to 1300 µS/cm.
Keywords: *E. coli*; aptamer; aptasensor; drinking water.

Resumen. En este trabajo, se diseñó y construyó un nuevo nanoaptasensor (NASEc) para la detección rápida y directa de *Escherichia coli* (*E. coli*) en agua potable. El sensor se basa en mediciones de conductividad eléctrica entre un conjunto de electrodos de oro sin modificar y un conjunto de electrodos de oro modificado. El conjunto de electrodos modificado se cubrió con una capa de aptámero (A_{E10}) para mejorar la afinidad por *E. coli* y una mejor unión a la superficie del electrodo. Utilizando la capa nanoestructurada modificada con nanotubos de carbono de paredes múltiples (MNTC) se logró la alta sensibilidad del sensor y permitió detectar la presencia de *E. coli* en cantidades de una sola unidad formadora de colonias (UFC) por 100 ml. Esta sensibilidad cumple con los estándares internacionales pertinentes de calidad del agua potable. Cada paso en el proceso de fabricación de NASEc fue verificado y probado mediante diferentes técnicas analíticas a nivel nanométrico y molecular: espectroscopia UV-vis y Raman, AFM y SEM. Este nanoaptasensor

J. Mex. Chem. Soc. **2025**, *69*(2)
Regular Issue

ISSN-e 2594-0317

portátil, simple y reutilizable con alta selectividad y afinidad ofrece una detección más rápida (3 min) en presencia de *E. coli* en comparación con los métodos convencionales basados en el recuento de unidades formadoras de colonias (UFC) (24 a 48 h). NASEc está diseñado para mediciones directas sin ningún tratamiento previo de muestras y es útil en agua potable dentro de un rango de conductividad de 50 a 1300 μS/cm.
Palabras clave: *E. coli*; aptámero; aptasensor; agua potable.

Introduction

Escherichia coli (E. coli) is a significant indicator of the microbiological quality of drinking water and is usually transmitted through the consumption of contaminated water or food [1]. Therefore, the presence of *E. coli* indicates faecal contamination [2], posing a health risk to individuals who consume such water [3,4]. Thus, water is constantly monitored by different International Regulatory Agencies such as the US Environmental Protection Agency (EPA) 2005, Ministere de la Santé 1996, Norma Oficial Mexicana modification NOM 127 SSA 1994, Word Health Organization (WHO) 1994, and Association Francaise de Normalisation (ANFOR) 1990. According to these agencies, the *E. coli* detection limit in drinking water must be zero CFU in 100 mL [4]. This means, detecting just one CFU in 100 mL makes it unsuitable for human consumption.

The colony-counting method has been used for detecting and quantifying *E. coli* in drinking water for decades [5]. This method involves several pre-steps such as cell culture with or without prior enrichment on a selective medium and requires characterization periods of 24 to 48 h [2,6]. In addition to the extended waiting period for results, it is also associated with challenges such as low sensitivity, antagonisms**,** and interferences with another bacterial source (low selectivity), poor detection of slow-growing bacteria, a necessity for sophisticated equipment, and highly educated personnel could be insolvencies present using this classic approach [2]. Nevertheless, this method is standardized and is the most used worldwide [7]. Therefore, it is not a surprise the growing interest in developing alternative methods for *E. coli* detection in drinking water, which will provide a simpler and shorter time of analysis, in compliance with all international standards in drinking water samples.

Table 1 shows different methods for *E. coli* detection in drinking water that were recently developed [3,7-10,12-24]. Some are very sophisticated and are based on electrochemical sensors (line 2 in table 1) [8], impedance spectroscopic or enzymatic sensors (lines: 10 to 13) [1–4], often using the modern knowledge of nanoscience and nanotechnology. While these methods require less time to detect *E. coli* compared to the colony-counting method (48 h) [11] they have very low sensitivity. None of the methods described in the first 13 lines were capable of detecting a single CFU 100 mL^{-1} . The methods reported in lines 14-16 were able to identify a single CFU100 mL^{-1}, but the analysis time was between 4 and 9 h. Finally, the method reported in line 17 had detected a single CFU 100 mL^{-1} in 15 min. However, they all require sophisticated instrumentation and laboratories for complex processes of preconcentration, incubation and qualified personnel**.**

In contrast, our nanoaptasensor (NASEc) could detect the presence of 1 CFU of *E. coli* in a sample volume of 100 mL within 3 min. As a result, our device is relatively simple, with high sensitivity, high selectivity, and reproducibility. The nanoaptasensor measures without the need for preconcentration or prior incubation which allows it to be used not only in laboratory settings but also for field measurements under various environmental conditions, without any limitation. It is easy to use and does not require any professional operator. As demonstrated in this work, the NASEc can be used in a reusable mode, which significantly reduces the cost of utilization. It is worth recalling that the methods mentioned in Table 1 a based on single-use sensors and imported with enzymatic electrodes/sensors are with very short time of activity. The first prototype of NASEc was used without any problem for 18 months.

J. Mex. Chem. Soc. **2025**, *69*(2)
Regular Issue

ISSN-e 2594-0317

Table 1. Methods for *E. coli* detection in drinking water.

No	Method detection	Sensitivity CFU/100 mL	Time	References
1	Organic / nanocomposite, resistance measurent	1 X10^7	17 h - 24 h	[12]
2	Aptasensor/ Chemiluminescent, aptamer- 6 FAM	4.5 X10^5	1 h	[13]
3	Microchip capillary electrophoresis/ specific aptamer	3.7 X10^4	20 min	[17]
4	Dip Test/ litmus paper with chemoattractant and enzymatic sustrate	2 X 10^4	75 min - 3h	[18]
5	Inmunosensor / Grafeno and AuNPs	1.5 X10^4	30 min	[3]
6	Microfluidic devise/ impedance measurements	< 10^4	15 -16 min	[19]
7	Glucometer/enzymatic activity	2 X 10^3	8 h	[20]
8	TaqMan - PCR	2 X 10^3	18 h	[21]
9	Smartphone/ µPad	1 X10^3	30 s	[22]
10	Biosensor platform µPad	1 X10^3	30-90 s	[9]
11	GUD Enzymatic detection / fluoresces	1 X10^3	20 - 120 min	[10]
12	Electrochemical detection / tyrosinase composite biosensors	1 X10^2	6.5 h	[8]
13	PCR - ELISA	5	4 h	[7]
14	Enzymatic Hydrolysis of 4-methylumbelliferone-B_D Galactoside	1	7 h	[23]
15	Detection B-galactosidase /chemiluminometric assay in cell permeabilized	1	6 - 9 h	[14]
16	Asytematic PCR/magnetic amperometric genosensors – AuSPE	1	4 h	[15,24]
17	Biosensor detection of B-D-galactosidase, electric GCE	1	15 min	[16]

Experimental

Reagents

The ssDNA aptamer (E10) for *E. coli* modified with -NH2 at the 3' end was used to build a modified electrode (A_{E10}), and was synthesized by Sigma-Aldrich Inc., USA [25].

The aptamer sequence is the following: 5'GCAATGGTACGGTACTTCCGTTGCACTGTGCGGCCGAGCTGCCCCCTGGTTTGTGAATACCCTGGGCAAAAGTGCACGCTACTTTGCTAA3'.

To prepare it for further use, it was dissolved in distilled water to create a stock solution of 114 µM.

Sodium dodecyl sulfate (SDS) and potassium chloride (KCl) were reactive grade (>99 %) and N-Hydroxysuccinimide (NHS) from Sigma–Aldrich Inc., México and 1 ethyl-dimethylaminopropil) carbodiimide and (EDC) from Life Technologies, Mexico City, Mexico

J. Mex. Chem. Soc. **2025**, *69*(2)
Regular Issue

ISSN-e 2594-0317

The multiwall carbon nanotubes (MWCNT) with a diameter of 20 – 40 nm and length of 10 – 30 μm with purity >95 wt % and ash <1.5 wt % were purchased from Cheaptubes Inc. Cambridgeport, VT, USA. Before modification with aptamers, the MWCNT (20 mg) was mixed with a 3:1 solution of sulfuric and nitric acids under continuous sonication for 2 h at 40 °C, centrifuged at 12,000 g for 20 min, and then washed twice with ultrapure water [26]. It was subsequently re-suspended in sodium dodecyl sulfate for additional sonication for 15 min. The suspension was centrifuged at 12,000 g for 30 min and washed twice with ultrapure water (Milli-Q, Millipore, USA). The resulting MWCNT-COOH was used for further modification with aptamers.

Bacterial culture isolation and preparation

E. coli strain was isolated from drinking water samples in Laboratory of Ambient Microbiology and Wastewater, UAM-l. The Serratia *marcescens* (*S. marcescens*) was obtained from the cultures the Faculty of Chemistry, Bacteriology Collection, UNAM. All bacterial cultures were checked for purity according to standard microbiological procedures. The conservation and propagation medium for *E. coli* and *S. marcescens* included: soy Agar and trypticasein, as well as liquid medium of soy broth. Agar Eosin and Methylene blue (EMB) were used for bacteria counting purposes.

Quantification of CFU 100 mL^{-1} by the membrane filtration technique

Quantified *E. coli* suspensions were prepared in 2.5 mM KCl solutions with a volume of 0.5 mL. Following an overnight culture of *E. coli* and centrifugation at 12000 g, for 15 min, the supernatant was discarded. The pellet was than resuspended in 1 mL of ultrapure sterile water (autoclaved 120 °C, 15 min) and washed once to remove the culture medium. The suspension's optical density was adjusted to ≥ 0.300 absorbance with a wavelength of 540 nm with a 2.5 mM KCl solution (autoclaved for 120 °C, 15 min) in 100 ml dilution bottles. Dilutions were filtered on a 0.45 μm membrane and placed in a differential (EMB) medium. Using the membrane filtration technique *E. coli* was quantified as colony forming units CFU 100 mL^{-1} [3,5].

Sample preparation for Raman and UV-Vis spectroscopies

Samples were prepared in 2 mL microcentrifuge tubes which contained solutions of A_{E10} (50,100, 250, 500, 2500, 5000 nM) and 1.5 mg mL^{-1} of MWCNT and the coupling reagents for the reaction: EDC, NHS in concentrations (0.4 M, 0.1 M). After mixing by sonification for 10 min, they were allowed to incubate 12 h and centrifuged at 12000 g for 20 min. Concentrations of A_{E10}, were calculated with the conversion factor of 1 OD 260 nM = 40 μg mL^{-1} of ssDNA, the difference between the value of A_{E10} in balance and the value of the initial concentration gives the values of complex A_{E10}–MWCNT solid phase. For immobilization of A_{E10} by covalent bonding, the procedure consisted of mixing 15μL (0.4M EDC) and 16μL (0.1M NHS) with 300 μL of A_{E10} (114 μM) and 15 μL of A_{E10} was applied to each electrode [27]. After 24 h, they were coated with Sigma brand mercaptoethanol (10 μL) and after 15 min, they were washed with distilled water to avoid nonspecific binding.

The Raman analysis of the NASEc surface with and without *E. coli*

Micro-Raman spectrometry (HoribaJohinYvon, T64000) was performed at room temperature with 532.1 nm and 20mW laser power at the output with 100X objective. 10 accumulations of 1 min per spectrum were performed. All Raman spectra were recorded at least three times in three different points of the sample, using an Olympus BX40 confocal microscope (Edison, NJ, USA). The spectra were calibrated using the 521 cm^{-1} line of monocrystalline silicon.

SEM analysis

The microscopic analysis of bacteria attached to biosensors was using a SEM Hitachi S-570. The surface of Au with MWCNT-A_{E10} and without A_{E10} was analyzed after being in the presence of 105 CFU 100 mL^{-1} *E. coli* and *S. marcescens*.

AFM characterization

The surface characterization with Atomic Force Microscopy (AFM) was carried out at room temperature and atmospheric conditions, with an AFM IV Microscope (Veeco Instruments Inc., USA) in tapping mode. The antimony (n) doped silicon probes with an average resonance frequency of 317 – 382 kHz with a spring constant of 20-80 N/nm were used at a scan rate of 0.4 – 0.7 Hz. The AFM acquisition was on 45 min average, in the height

J. Mex. Chem. Soc. **2025**, *69*(2)
Regular Issue

ISSN-e 2594-0317

and phase mode. All image analyses were performed using the AFM NanoScope software. Each sample was examined at five different places over the surface in two different series of measurements.

Conductivity analysis system

The conductivity measurements were carried out with Hanna Instruments multiparametric pH/mV/°C/CE/TDS HI255.

Statistical analysis

To determine the difference between the treatments with and without *E. coli*, analysis of variance and multiple mean comparisons (Duncan and Tukey) were performed for a significance level (α) of 0.05. The analysis was carried out with Minitab 18.

Results

Design and construction of NASEc

We designed and constructed a highly sensitive sensor surface (electrodes of 5 mm diameter and 19.6 mm^2 surface, circle) with high affinity for *E. coli* bacteria. This was achieved by using special aptamers (A_{E10}) fixed at the electrode, then we modified the electrode surface with carbon nanotubes (MWCNT) for bacterial attachment see Fig. 1**(A)** (a-c).

The NASEc is form by two pairs in parallel positioned electrodes. The first set is assembled from two bare gold (Au) electrodes and the second one consists of two gold modified by MWCNT and aptamers (Au-MWCNT-A_{E10}) as seen in Fig. 1**(A)**d. To develop a highly efficient sensor, we adhered to a validated nanostructuring and to nanomodification process (details are presented in the methodology part of this paper and a patent [28]). Then, the sensor surface was analyzed by the following techniques: UV-vis and Raman Spectroscopy, Atomic Force Microscopy (AFM), and Scanning Electron Microscopy (SEM).

Attachment of A_{E10} on MWCNT

Fig. 1**(B)** shows the results of the affinity test of A_{E10} towards the MWCNT. A series of A_{E10} solutions (3.0 µg mL^{-1} – 115.0 µg mL^{-1}) were aggregated in a vial with a constant concentration of MWCNT (1.5 mg mL^{-1}). Following 48 h of equilibrium, part of the aptamers reacted with MWCNT, and the rest of the non-coupled were measured with UV-vis Spectroscopy. Our data showed a saturation effect, after the concentration reached 40 to 60 µg mL^{-1},MWCNT. Other authors [29-31] show data about the affinity between single-wall carbon nanotubes (SWCNT) and aptamer AE22 P2 and conclude that saturation occurs at 120 µg mL^{-1} for 500 nM of SWCNT.

Similar data were obtained by other authors [32]. However, many authors demonstrate that saturation could vary in the function of the CNT used and methods of preparation (chemical vs. physical adsorption).

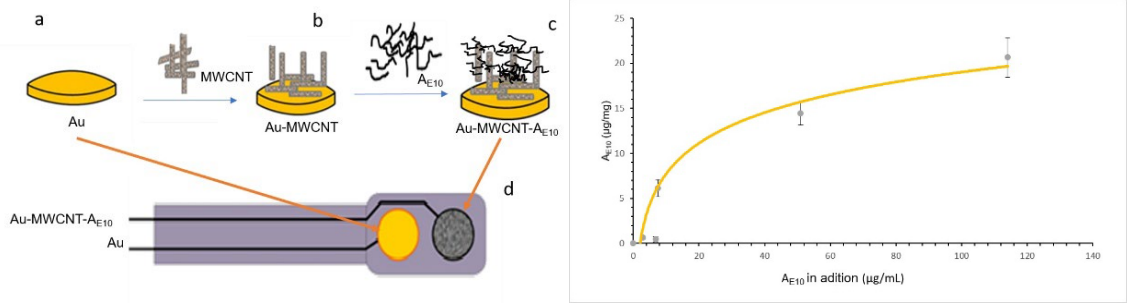

Fig. 1. (A) Schematic presentation of the NASEc fabrication. **(B)** Affinity plot for A_{E10} towards MWCNT.

Raman analysis

Raman Spectroscopy was also used for the characterization of the functionalized NASEc. Fig. 2**(A)** shows the typical spectra of the MWCNT electrode surface before and after functionalization with A_{E10}. The

J. Mex. Chem. Soc. **2025**, *69*(2)
Regular Issue

ISSN-e 2594-0317

Raman peaks observed at 1342 cm^{-1} (D) and 1577 cm^{-1} (G) [33] are related to the C-C longitudinal vibrations: peak D with carbon amorphous (disorder) and peak G with ordered graphitic part of CNT. On the other hand, A_{E10} does not show any Raman peak by itself, probably due to a very small concentration. However, we observed that the intensity between peaks D and G changes as a function of the modification by $\mathbf{A_{E10}}$. Raman spectra obtained for MWCNT film without A_{E10} (Fig. 3), with 14 µg/mL, and with 139 µg mL^{-1} of A_{E10} show different intensity between the D and G peaks.

Therefore, these peaks were used to monitor the process of MWCNT modification. The ratio between the intensity of G/D peaks is plotted in Fig. 2**(B)**. Peak G increases by modification of MWCNT with A_{E10}, which could be a result of better ordering at the surface sample due to adsorption of highly ordered aptamer molecules [34].

Fig. 3 shows the typical Raman spectra of the MWCNT film functionalized with A_{E10} (NASEc) and exposed to an *E. coli* sample. This results in the appearance of many new peaks in the range of 400–1800 cm^{-1}, bands due to DNA (701 and 747 cm^{-1}), amide III (1262 cm^{-1}), CH deformation of the lipids of the *E. coli* membrane (1437 cm^{-1}), and tryptophan (1540 cm^{-1}) [35,36] related to the functional groups at the bacteria surface.

The Amide I band is observed as a shoulder on the higher frequency side of the NTC G band. For assignation one could check in the literature mentioned [17,37–39]. These results clearly show that *E. coli* is fixed on the electrode surface.

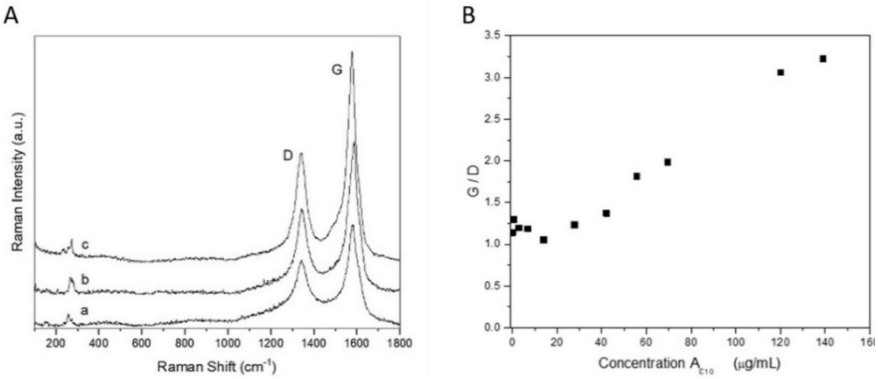

Fig. 2. (A) Raman spectra of the MWCNT samples: without (a), after modified with 14 µg/mL (b) and modified with 139 µg mL-1 of A_{E10} (c). Raman peeks characteristic for MWCNT could be seen at 1342 cm^{-1} (D) and 1577 cm^{-1} (G). **(B)** The ratio G/D peaks for MWCNT modified by different concentration of A_{E10}.

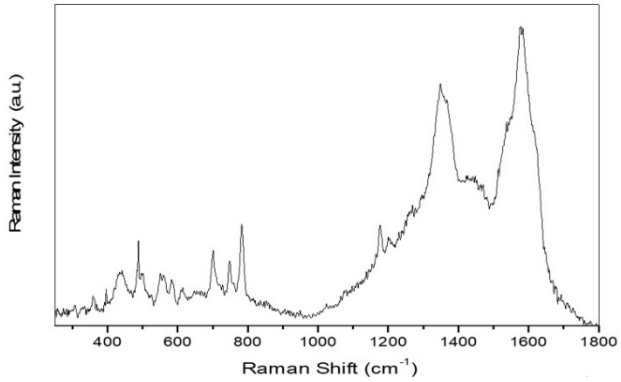

Fig. 3. Typical Raman spectra of the MWCNT film functionalized with A_{E10} (NASEc sensor) and exposed to an *E. coli* sample.

The AFM and SEM Analysis

Besides those indirect methods, AFM and SEM were used to see the modification of the electrode surface by A_{E10} and to identify the *E. coli* presence. AFM was used to analyze the topography properties of the non-modified and A_{E10} modified MWCNT. Fig. 4**(a-f)** shows a top view image (a and d), a cross-section

J. Mex. Chem. Soc. **2025**, *69*(2)
Regular Issue

ISSN-e 2594-0317

analysis (b and e), and a 3D view (c and f). The images a,b and c correspond to a non-modified bare MWCNT sample and images d,e and f are MWCNT modified with A_{E10}. The high-resolution images were obtained from the electrode surface (600 x 600 nm), and we observed a significant difference in the diameter and form of the MWCNTs features. The results of the quantitative analysis at the nanometric scale showed that Au-MWCNT feature diameter is in average 40.43 +/- 6.03 nm, and Au-MWCNT-A_{E10} about 62.52 +/- 8.10 nm. Finally, the MWCNT diameter increased by adsorption of the aptamers, which supports and confirms the successful modification of the electrode surface by aptamers molecules [40,41]**.**

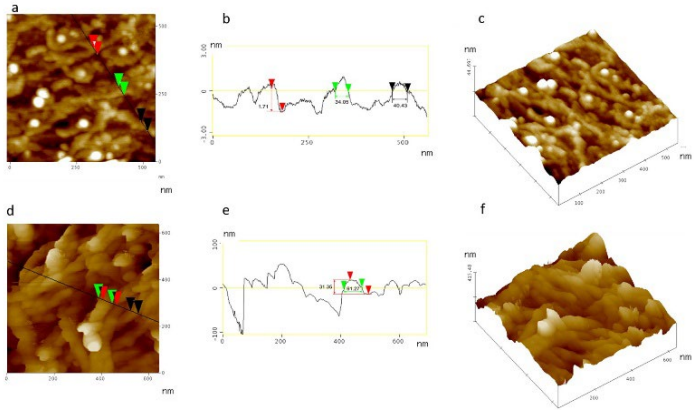

Fig. 4. High resolution AFM images show MWCNT before **(a, b, c)** and after modification by A_{E10} **(d, e, f)**. Mode of presentation: Top–view (a and d), cross-section analysis (b and e) and 3D view (c and f).

The step further in the characterization of the NASEc surface was achieved using SEM. In Fig. 5**(a-c)**, we observed the distribution of MWCNT-A_{E10} on the Au-electrode surface. Almost the whole electrode surface is uniformly and fully covered by MWCNT-A_{E10} features. Thus, well distributed, and closely packed A_{E10} provides more efficient adsorption and interaction of *E. coli* with the modified surface. Fig. 5 (b and c) show a set of SEM micrographs of the MWCNT-A_{E10} surface in the presence of *E. coli* obtained at different magnifications**.**

The high-resolution micrograph allowed us the identification of individual MWCNT-A_{E10} and *E. coli* bacteria (1.5 µm to 2 µm in diameter) at the sample surface [42–44]. Since the sensor was exposed to a very high bacterial concentration: $1x10^5$ CFU 100 mL^{-1}, the surface density of the bacterial film was high. It seems a closely packed film spread all over the sensor surface (Fig. 5**(c)**). The bacterial film is disordered and presumably formed following some kind of instantaneous mechanism, which means primary adsorption is controlled by strong interaction between the surface-attached aptamers and bacterial surface [42].

We also conducted adsorption of the bacteria *S. marcescens* on the same electrode surface. The SEM micrographs showed that within the same experimental conditions: bacterial concentration, temperature, time of sensor exposure to the bacterial media, the *S. marcescens* does not show any form of interaction with our sensor. The surface remained clean Fig. 5**(d-e)** with no presence of bacteria. According to the literature, *S. marcescens* does not have an affinity to the surface of our sensor, which supports our conclusion about the high selectivity of the NASEc sensor for *E. coli.* To determine the presence of E. coli in the water sample, two electrodes with two sets of Au-electrodes and Au-MWCNT-AE10 were connected in separate electrical circles to measure conductivity (Fig. 6).

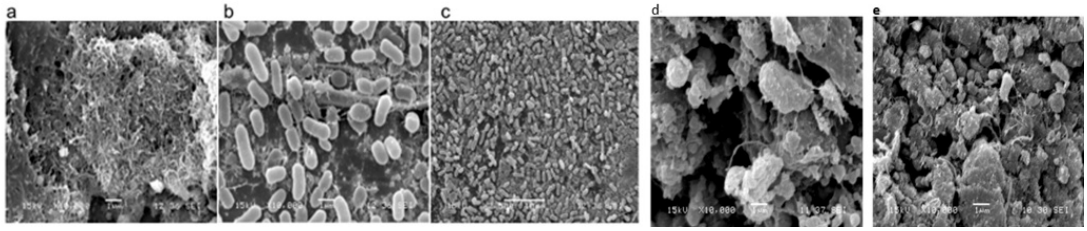

Fig. 5. SEM micrographs show: MWCNT-A_{E10} surface before **(a)** and after *E. coli* adsorption **(b)** and **(c)**, which different amplification. SEM micrographs of the NASEc surface: before **(d)** and after **(e)** exposing to *S. marcescens* bacteria, show low affinity.

J. Mex. Chem. Soc. **2025**, *69*(2)
Regular Issue

ISSN-e 2594-0317

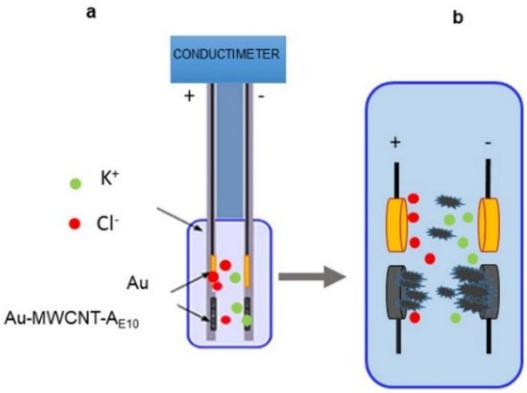

Fig. 6. Schematic representation of the NASEc function (conductivity measurements).

Mechanism of *E. coli* detection in drinking water samples by electrolytic conductivity measurements

To determine the presence of *E. coli* in the water sample, two electrodes with two sets of Au-electrodes and Au-MWCNT-A_{E10} were connected in separate electrical circles to measure conductivity.

The electrodes were placed at a fixed distance of 3 mm from each other and connected to a commercial conductivity meter (Model H I98312, Hanna Instruments Inc., USA). The conductivity between the two electrodes is a function of the concentration of ions in the solution, as presented in Fig. 7**(a)**. Consecutively, we were able to measure the conductivity between the two Au electrodes (C_{Au}) and between the two modified electrodes (C_{Au}-MWCNT-A_{E10}).

When *E. coli* is present in water, the bacteria have a high affinity towards the aptamer-modified electrode surface and preferentially and exclusively adsorbs on the Au-MWCNT-A_{E10} electrodes without interfering with the bare Au surface. Due to the adsorption and covalent bonds of *E. coli* on the modified-electrode surface, the ion flow from the solution to the modified electrode surface is obstructed and inhibited, resulting in a decrease in the conductivity value. This inhibition effect for *E. coli* is present only in the A_{E-10}-modified electrodes (Fig. 7**(b)**). To continue with a systematic approach and obtain reliable results, we used the same distance between the pair of electrodes, the same sample temperature range (23 – 24 °C), and the same measurement time (3 min). Data is given later in the text.

The first experiments with NASEc involve the probe with KCl solution, as a model system, in the concentration range from 1 to 10 mM. Fig. 7**(a)** shows the conductivity values of Au-MWCNT-A_{E10} (I) and Au (II) electrodes, respectively. We observed that the conductivity increases with the concentration of KCl in the solution. The increase is linear as seen from the following data: Y = 104.52x + 23.605, R2 = 0.9972 and Y= 71.499x + 5.6627 with R2 = 0.9952, for Au-MWCNT-A_{E10} (I) and Au (II) electrode, respectively. The conductivity values for Au-MWCNT-A_{E10} are higher than those for Au electrodes due to larger active surface area in the modified electrodes enhanced by the MWCNT modification. The tendency between these two curves is progressive, higher differences are observed at higher KCl concentrations. The curve (III) represents the difference (ΔC) between the conductivity measurements with Au-CNT-A_{E10} (I) and Au (II) electrodes and shows the same characteristics as those previously described (Y= 33.022 x + 17.942 with R2 = 0.9972).

$$\Delta C = (C_{Au}\text{-MWCNT-}A_{E10}) - (C_{Au}) \quad (1)$$

Thus, *E. coli* does not adsorb at the bare Au electrodes and selectively shows high affinity for the Au-MWCNT-A_{E10} electrode surface, obstructing the contact between the ionic species and Au-MWCNT-A_{E10} electrodes. Therefore, the conductivity of the modified electrodes decreased. As demonstrated before, this will impact the ΔC value.

Before this calibration, a series of measurements were carried out to determine the correct response time of the aptasensor in a range of 0 to 5 min. After 2 to 3 min the response was stable, which means that

J. Mex. Chem. Soc. **2025**, *69*(2)
Regular Issue

ISSN-e 2594-0317

equilibrium between the solid electrode layer and the solution was established (Fig. 7**(b)**). Carrying out the conductivity measurements within 3 min of the equilibrium time was sufficient to obtain reproducible results.

The values reported for C_{Au} are different from those reported in the literature for the same system (the same concentrations of KCl) [45]. This is due to the different physical characteristics of the sensor. Commercial sensors are standardized and calibrated differently than our sensors.

However, we also performed a standard measurement test for KCl solutions with commercial and well-calibrated instrumentation. With a standard conductometer, we tested a set of samples from 100 to 1300 µS cm^{-1} (the expected range for drinking water samples), and NASEc showed 100 to 700 µS cm^{-1}.

The differences obtained are preferably due to different electrode sizes (area) and electrode separation distances between these two instruments. The measurements were limited to the Au electrodes since the commercial sensor does not have an option for the A_{E10}-modified electrodes. Moreover, Fig. 7**(c)** shows values for ΔC_{Au} obtained with a standardized commercial sensor (I) and NASEc (II) for samples with same KCl concentration. In both cases, the relation between the ΔC_{Au} and KCl concentration is linear.

Therefore, values obtained by NASEc could be easily standardized. In order to facilitate the use of our sensor, we developed an algorithm based on the relation between ΔC vs. C_{Au}. The ΔC vs. C_{Au} plot is presented in Fig. 7**(d)**, which means that for each C_{Au} there is a ΔC value assigned. The data in this graph was obtained using previously sterilized KCl solution and prepared for *E. coli* addition. As we noticed this process could cause variation in the C_{Au} conductivity in the range of ± 5 %. Using this graph, we observed that for C_{Au}= 100 µS cm^{-1}, the corresponding value of ΔC is 90 µS cm^{-1}, and for C_{Au}= 522 µS cm^{-1}, ΔC is 272 µS cm^{-1}.

Fig. 8 shows changes in ΔC vs. C_{Au} obtained for a very small and narrow range around 2.5 mM KCl solutions with different content of *E. coli* (0, 1, 2, and 4 CFU). As described before in the methodology, the samples for this test were prepared by dilution of highly content *E coli* suspension. The dilution process was used to obtain samples with a very small number of CFU 100 mL^{-1}. After each step, the value of CFU was checked by the classical method of CFU evaluation. Note that 0 CFU 100 mL^{-1} means that by classical methods no CFU 100 mL^{-1} was detected. It still does not mean that the sample does not have *E. coli* in form of individual bacteria. Such observation is confirmed in our preliminary studies in laboratory conducted by Flow Cytometry method. Since NASEc is a sensor for CFU determination, in this paper we did not pay special attention to those findings.

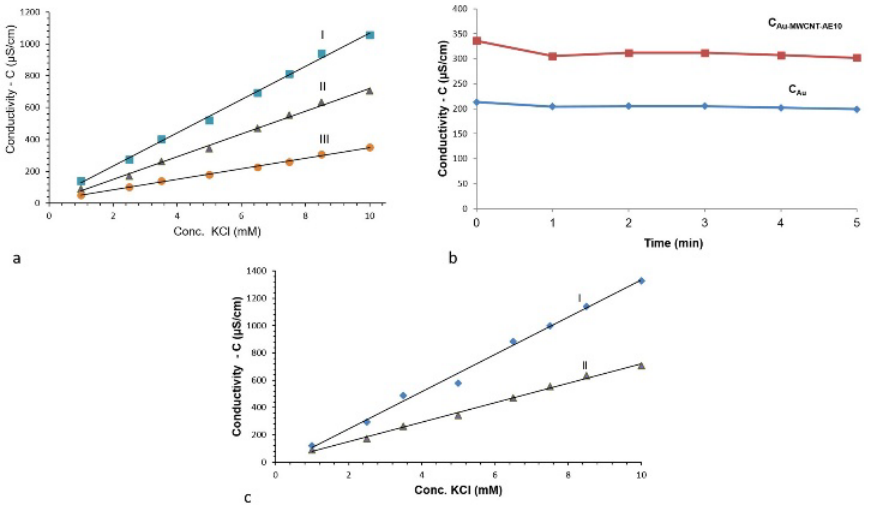

Fig. 7. (a) Conductivity vs. KCl concentration obtained with NASEc for: CAu-MW-NTC-A_{E10} (I), C_{Au} (II) and ΔC (III), respectively. **(b)** Stability of NASEc measurements obtained during first 5 min of use. **(c)** Values for C_{Au} obtained with standardized commercial sensors (I) and NASEc (II) for samples with the same KCl concentration.

To evaluate and calibrate the influence of *E coli* on the ΔC value measured by NASEc, all readings are conducted at a single C_{Au} value (205 µS cm^{-1}). As expected, the presence and increase of *E. coli* reduced ΔC, at least in the range of 1 to 4 CFU 100 mL^{-1} of *E. coli*. At the higher presence of *E. coli* in samples (4 < CFU 100 mL^{-1} <20), the values of ΔC are almost constant or even slightly increasing, which indicates the sensor saturation. As seen in Fig.

J. Mex. Chem. Soc. **2025**, *69*(2)
Regular Issue

ISSN-e 2594-0317

8, (ΔC vs. CFU 100 mL^{-1} plot) NASEc could efficiently distinguish the presence of 1, 2, 3 or 4 CFU 100 mL^{-1}, vs. no presence (0 CFU) in the 0.25 mM KCl. This graph (Fig. 8) could serve for the determination of CFU of E. *coli* in drinking water samples.

Again, to determine if drinking water meets bacteriological standards (*E coli* content = 0 CFU 100 mL^{-1}) and is suitable for human use, it is sufficient to immerse NASEc in 100 mL of sample and wait 3 min. After measuring the electrical conductivity of the set of Au electrodes (C_{Au}) and the set of Au-MWCNT-A_{E10} (C_{Au}MWCNT-$_{AE10}$), calculate $\Delta C_{experimental}$ value and compare it with expected $\Delta C_{calibration}$ value obtained in the calibration process. The decrease in the ΔC value will be an indicator of the *E. coli* presence in the water and should be discarded for drinking.

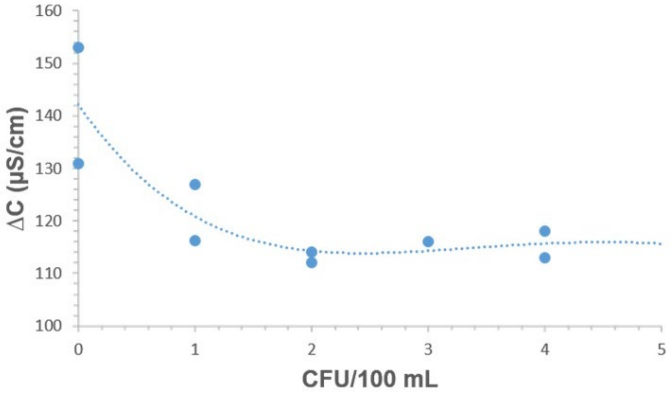

Fig. 8. ΔC vs. CFU 100 mL^{-1} of *E. coli*, calibration curve.

NASEc stability

One of the advantages of using aptamers for electrode modification over antibodies is their structural stability and durability, which significantly increase the electrode life.

To evaluate the stability of the modified nanostructure surface and the NASEc stability, a test over two years with 30 experiments was performed. In all cases, the sensor was tested with 2.5mM KCl solution at 24 °C without *E. coli*. Results are presente in Fig. 9. Two parameters were measured each time: C_{Au} (II) and $C_{Au\text{-}NTC\text{-}AE10}$ (I). Indeed, NASEc shows great stability and consistency during the whole test. The values for C_{Au} were 189 (sd=22) µS cm^{-1} average, and for C_{Au}-MWCNT-A_{E10} were 32 (sd=26) µS cm^{-1}.

Interestingly in some cases, the same test was performed just after using the sensor in the *E. coli* suspension. See marks: 1-8 at the top of the graph in Fig. 9. It did not change the distribution of results, indicating the reuse of the NASEc. Furthermore, it is well known that immobilization carried out between MWCNT-aptamer conjugates demonstrates the prolonged half-life of aptamers [46].

The robustness and stability combined with the reusability of our sensor make it suitable for cost-effective use, which is an important characteristic for the manufacture of aptasensors.

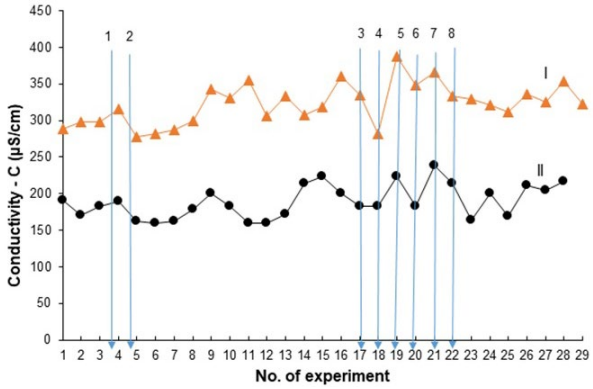

Fig. 9. Test of stability and reproducibility of NASEc.

J. Mex. Chem. Soc. **2025**, *69*(2)
Regular Issue

ISSN-e 2594-0317

Conclusions

An aptasensor (NASEc) capable of detecting *E. coli* in water at levels of 1 CFU 100 mL^{-1} was developed. Hence, an Au electrode was modified with MWCNT and functionalized with an A_{E10} aptamer. Based on the measurement of electrolytic conductivity between the two electrodes, it could easily and quickly register the presence of *E. coli* in a drinking water sample. NASEc is the product of highly sophisticated knowledge in of nanotechnology, microbiology, and biotechnology. During the construction, each component was carefully tested by different techniques: AFM, Raman Spectroscopy, and SEM. In this way each step of assembling was studied in detail and with great understanding. It started from the analysis and characterization of MWCNT via functionalization by A_{E10} aptamer to the detailed characterization of fully assembled electrodes. The main characteristics of NASEc are high sensitivity (single CFU 100 mL^{-1}), fast response (3 min), portability, high selectivity, high Apastability, and reusability. It offers a clear advantage compared to traditional techniques and in the future, it could be a preferred tool (an alternative method) for the detection of *E. coli* in drinking water, and overall assessment of drinking water quality concerning bacterial contamination in homes, distribution network, and during the water purification processes.

Acknowledgements

Dr. Jose Sepulveda y Dra. Ma. Cristina Acosta for the SEM micrographs. This study was supported by SEM; SECITI of the GDF for the financing of the project SECITI 054/2013 "Sensor Doméstico de calidad de agua"; CONACyT for the Doctorate scholarship (No. 100414) warded to E.V.M., and for the Posgrado en Biotecnología (Ref. 001466).

References

1. Zhao, Y. W.; Wang, H. X.; Jia, G. C.; Li, Z. *Sensors*. **2018**, *18*, 1–16. DOI: https://doi.org/10.3390/s18010318.
2. Rompré, A.; Servais, P.; Baudart, J.; De-Roubin, M. R.; Laurent, P. *J. Microbiol. Methods*. **2002**, *49*, 31–54. DOI: https://doi.org/10.1016/S0167-7012(01)00351-7.
3. Khan, F. M.; Gupta, R.; Sekhri, S. *Environ. Sci. Pollut. Res.* **2021**, *28*, 60778-60786. DOI: https://doi.org/10.1007/s11356-021-14983-3.
4. Wu, W.; Li, M.; Wang, Y.; Ouyang, H.; Wang, L.; Li, C.; Cao, Y.; Meng, Q.; Lu, J. *Nanoscale Res. Lett.* **2012**, *7*, 658. DOI: https://doi.org/10.1186/1556-276x-7-658.
5. Eaton, A. D.; Clesceri, L. S.; Rice, E. W.; Greenberg, A. E.; Franson, M. A. H., in: *Standard Methods for the Examination of Water and Wastewater,* 21st ed., American Public Health Association, Washington, DC, **2005**.
6. Walker, D. I.; McQuillan, J.; Taiwo, M.; Parks, R.; Stenton, C. A.; Morgan, H.; Mowlem, M. C.; Lees, D. N. *Water Res*. **2017**, *126*, 101–110. DOI: https://doi.org/10.1016/j.watres.2017.08.032.
7. Kuo, J. T.; Cheng, C. Y.; Huang, H. H.; Tsao, C. F.; Chung, Y. C. J. *Ind. Microbiol. Biotechnol.* **2010**, *37*, 237–244. DOI: https://doi.org/10.1007/s10295-009-0666-0.
8. Serra, B.; Morales, M. D.; Zhang, J.; Reviejo, A. J.; Hall, E. H.; Pingarron, J. M. *Anal. Chem*. **2005**, *77*, 8115–8121. DOI: https://doi.org/10.1021/ac051327r.
9. Ionescu, R. E. *Escherichia coli: Recent Adv. Physiol., Pathog. Biotechnol. Appl.* **2017**. DOI: https://doi.org/10.5772/67392.
10. Hesari, N.; Alum, A.; Elzein, M.; Abbaszadegan, M. *Enzyme Microb. Technol.* **2016**, *83*, 22–28. DOI: https://doi.org/10.1016/j.enzmictec.2015.11.007.
11. Jiang, Y. S.; Riedel, T. E.; Popoola, J. A.; Morrow, B. R.; Cai, S.; Ellington, A. D.; Bhadra, S. *Water Res.* **2018**, *131*, 186–195. DOI: https://doi.org/10.1016/j.watres.2017.12.023.

J. Mex. Chem. Soc. **2025**, *69*(2)
Regular Issue

ISSN-e 2594-0317

12. Mallya, A. N.; Sowmya, P.; Ramamurthy, P. C., in: *Organic Nanocomposite Sensor for Detection of Escherichia coli*, 2014 IEEE 2nd International Conference on Emerging Electronics (ICEE), Bengaluru, India, **2014**.
13. Khang, J.; Kim, D.; Chung, K. W.; Lee, J. H. *Talanta*. **2016**, *147*, 177–183.
14. Van Poucke, S. O.; Nelis, H. *Appl. Environ. Microbiol.* **1995**, *61*, 4505–4509. DOI: https://doi.org/10.1128/aem.61.12.4505-4509.1995.
15. Loaiza, Ó. A.; Campuzano, S.; Pedrero, M.; García, P.; Pingarrón, J. M. *Analyst*. **2009**, *134*, 34–37. DOI: https://doi.org/10.1039/b815307h.
16. Wutor, V. C.; Togo, C. A.; Limson, J. L.; Pletschke, B. I. *Enzyme Microb. Technol.* **2007**, *40*, 1512–1517.
17. Su, L.; Zhang, P.; Zheng, D.; Wang, Y.; Zhong, R. *Optoelectron. Lett.* **2015**, *11*, 157–160.
18. Gunda, N. S. K.; Dasgupta, S.; Mitra, S. K. *PLOS ONE*. **2017**, DOI: https://doi.org/10.1371/journal.pone.0183234.
19. Zuo, P.; Li, X.; Dominguez, D. C.; Ye, B. C. *Lab Chip*. **2013**, *13*, 3921–3928. DOI: https://doi.org/10.1039/c3lc50654a.
20. Mitra, S. *Anal. Methods*. **2014**, *6*, 6236–6246.
21. Frahm, E.; Obst, U. *J. Microbiol. Methods*. **2003**, *52*, 123–131. DOI: https://doi.org/10.1016/s0167-7012(02)00150-1.
22. McCracken, K. E.; Angus, S. V.; Reynolds, K. A.; Yoon, J. Y. *Sci. Rep.* **2016**, *6*, 1–13.
23. Berg, J. D.; Fiksdal, L. *Appl. Environ. Microbiol.* **1988**, *54*, 2118–2122. DOI: https://doi.org/10.1128/aem.54.8.2118-2122.1988.
24. Sun, H.; Choy, T. S.; Zhu, D. R.; Yam, W. C.; Fung, Y. S. *Biosens. Bioelectron.* **2009**, *24*, 1405–1410. DOI: https://doi.org/10.1016/j.bios.2008.08.008.
25. Kim, Y. S.; Song, M. Y.; Jurng, J.; Kim, B. C. *Anal. Biochem.* **2013**, *436*, 22–28. DOI: https://doi.org/10.1016/j.ab.2013.01.014.
26. Evtugyn, G.; Porfireva, A.; Ryabova, M.; Hianik, T. *Electroanalysis*. **2008**, *20*, 2310–2316. DOI: https://doi.org/10.1002/elan.200804345.
27. Téllez-Plancarte, A.; Haro-Poniatowski, E.; Piquart, M.; Morales-Méndez, J. G.; Lara-Cruz, C.; Jiménez-Salazar, J. E.; Damian-Matsumura, P.; Escobar-Alarcón, L.; Batina, N. *Nanomaterials*. **2018**, *8*, 549. DOI: https://doi.org/10.3390/nano8070549.
28. Gómez-Reyes, A. R. E.; Monroy, O. A.; Batina, N.; Jiménez, D.; Abad, A. R.; Constantino, R.; Montero, D. P.; Tapia, F. O.; Ramírez, F.; Velázquez, E.; Morales, I.; Hernández, P.; Solís, A.; Hernández, J. de J. *Mex. Pat.*, **2021**.
29. Zhang, S.; Wang, X.; Li, T.; Liu, L.; Wu, H. C.; Luo, M.; Li, J. *Langmuir*. **2015**, *31*, 10094–10099. DOI: https://doi.org/10.1021/acs.langmuir.5b01272.
30. Ozkan-Ariksoysal, D.; Kayran, Y. U.; Yilmaz, F. F.; Ciucu, A. A.; David, I. G.; David, V.; Hosgor-Limoncu, M.; Ozsoz, M. *Talanta*. **2017**, *166*, 27–35. DOI: https://doi.org/10.1016/j.talanta.2017.01.005.
31. Yang, M.; Peng, Z.; Ning, Y.; Chen, Y.; Zhou, Q.; Deng, L. *Sensors*. **2013**, *13*, 6865–6881. DOI: https://doi.org/10.3390/s130506865.
32. Ocaña, C.; Pacios, M.; del Valle, M. *Sensors*. **2012**, *12*, 3037–3048. DOI: https://doi.org/10.3390/s120303037.
33. Murphy, H.; Papakonstantinou, P.; Okpalugo, T. I. T. *J. Vac. Sci. Technol., B: Microelectron. Nanometer Struct. --Process., Meas., Phenom.* **2006**, *24*, 715–720.
34. Le, V. T.; Ngo, C. L.; Le, Q. T.; Ngo, T. T.; Nguyen, D. N.; Vu, M. T. *Adv. Nat. Sci. Nanosci. Nanotechnol.* **2013**, *4*, 4–9.
35. Maquelin, K.; Kirschner, C.; Choo-Smith, L.-P.; Ngo-Thi, N. A.; van Vreeswijk, T.; Stämmler, M.; Endtz, H. P.; Bruining, H. A.; Naumann, D.; Puppels, G. J. *J. Clin. Microbiol.* **2003**, *41*, 324–329. DOI: https://doi.org/10.1128/jcm.41.1.324-329.2003.
36. Wu, Q.; Hamilton, T.; Nelson, W. H.; Elliott, S.; Sperry, J. F.; Wu, M. *Anal. Chem.* **2001**, *73*, 3432–3440. DOI: https://doi.org/10.1021/ac001268b.

J. Mex. Chem. Soc. **2025**, *69*(2)
Regular Issue

ISSN-e 2594-0317

37. Sengupta, A.; Mujacic, M.; Davis, E. J. *Anal. Bioanal. Chem.* **2006**, *386*, 1379–1386. DOI: https://doi.org/10.1007/s00216-006-0711-z.
38. Zainudin, N.; Mohd Hairul, A. R.; Yusoff, M. M.; Tan, L. L.; Chong, K. F. *Anal. Methods.* **2014**, *6*, 7935–7941. DOI: https://doi.org/10.1039/C4AY01836B.
39. Athamneh, A. I. M.; Alajlouni, R. A.; Wallace, R. S.; Seleem, M. N.; Sengera, R. S. *Antimicrob. Agents Chemother.* **2014**, *58*, 1302–1314. DOI: https://doi.org/10.1128/aac.02098-13.
40. Guler, Z.; Sarac, A. S. *eXPRESS Polym. Lett.* **2016**, *10*, 96–110.
41. Lian, Y.; He, F.; Wang, H.; Tong, F. *Biosens. Bioelectron.* **2015**, *65*, 314–319.
42. Upadhyayula, V. K. K.; Deng, S.; Mitchell, M. C.; Smith, G. B. *Sci. Total Environ.* **2009**, *408*, 1–13. DOI: https://doi.org/10.1016/j.scitotenv.2009.09.027.
43. Radke, S. M.; Alocilja, E. C. *Biosens. Bioelectron.* **2005**, *20*, 1662–1667. DOI: https://doi.org/10.1016/j.bios.2004.07.021.
44. García-Aljaro, C.; Cella, L. N.; Shirale, D. J.; Park, M.; Muñoz, F. J.; Yates, M. V.; Mulchandani, A. *Biosens. Bioelectron.* **2010**, *26*, 1437–1441. DOI: https://doi.org/10.1016/j.bios.2010.07.077.
45. Demattê, J. A. M.; Ramirez-Lopez, L.; Marques, K. P. P.; Rodella, A. A. *Geoderma*. **2017**, *288*, 8–22.
46. Hayat, A.; Marty, J. L. *Front. Chem.* **2014**. DOI: https://doi.org/10.3389/fchem.2014.00041.